The colour of sulphur

1998 J. Phys.: Condens. Matter 10 4093

(http://iopscience.iop.org/0953-8984/10/18/018)

J. Phys.: Condens. Matter **10** (1998) 4093–4100. Printed in the UK PII: S0953-8984(98)89439-3

The colour of sulphur

O V Krasovska†, B Winkler†, E E Krasovskii‡, V N Antonov‡ and B Yu Yavorsky‡

† Mineralogisch-Petrographisches Institut der Christian-Albrechts Universität, Olshausenstrasse 40, D 24098 Kiel, Germany

‡ Institute of Metal Physics, National Academy of Sciences of Ukraine, Vernadskogo 36, 252680, Kiev-142, Ukraine

Received 21 November 1997, in final form 11 February 1998

Abstract. Optical properties of a trigonal polymorph of sulphur are explained in terms of the electronic energy band structure. The electron states of sulphur are obtained using the *ab initio* semi-relativistic extended linear augmented-plane-wave method (ELAPW). The density-of-states spectrum of the valence band is in agreement with x-ray photoemission, Kβ and $L_{II,III}$ x-ray emission spectra. The calculated polarized optical spectra are in satisfactory agreement with the experimental reflectivity spectra. All of the structures in the experimentally determined optical spectra in the energy region $0 \leqslant \hbar\omega \leqslant 15$ eV are interpreted in terms of interband p $\rightarrow$ p transitions.

1. Introduction

The colour of a perfect crystalline dielectric is due to optical transitions of valence electrons to the conduction band. The minimal photon energy at which such transitions are allowed, the absorption threshold, is the width of the direct forbidden gap of an insulator or semiconductor. Thus, in the case where the onset of the optical absorption falls into the visible photon energy range, the colour of the crystal is determined by the photon energy of the absorption threshold and by the spectral distribution of the intensity of the transitions.

In this paper we explain the colour of sulphur in terms of a mechanism analogous to the d $\rightarrow$ d transitions in the 3d metal containing salts and oxides [1, 2]. There the interaction of the 3d ion with its environment makes transitions between occupied and unoccupied atomic-like 3d states possible. In sulphur the electron states in both the occupied and unoccupied parts of the 3p band retain localized atomic character. For this reason we call the dipole transitions between them p $\rightarrow$ p transitions to emphasize the distinction from the charge-transfer transitions, where the optical transitions are between the states localized at different atoms or between a localized and a delocalized state. The effect of the crystalline environment is much stronger in the case of p states than the crystal-field interaction in the 3d-transition-metal-containing compounds; consequently the absorption is several orders of magnitude larger.

The reflectivity spectra of sulphur in the visible and ultraviolet region have been measured by Spear and Adams [3] and Cook and Spear [4] using unpolarized light. Polarized reflectivity measurements have been presented by Emerald *et al* [5]. Absorption measurements have been performed by Spear and Adams [3], and the pressure dependence of the fundamental absorption edge has been presented by Peanasky *et al* [6] for pressures

0953-8984/98/184093+08$19.50

up to 300 kbar. Knowledge of the optical constants of elementary sulphur was crucial in the determination of the surface constituents of Venus, Jupiter and Io during the Voyager flight. This stimulated a series of ellipsometrical measurements of solid and liquid sulphur [7]. A good deal of information about the optical properties has been obtained from these experiments, but no definite conclusion as to the origin of the features observed in the optical spectra has been reached. In the present work we suggest an explanation of the optical properties of sulphur in terms of the electronic energy band structure.

An unambiguous interpretation and assignment of the experimentally observed spectral features to specific electronic excitations in the Brillouin zone requires accurate electronic structure calculations. Most of the accurate present-day *ab initio* calculations are based on density-functional theory (DFT) [8]. For the calculations of ground-state properties of an electronic system, the most important approximation within the DFT used to construct the one-electron potential is the local density approximation (LDA) [9]. However, in the case where excited states are involved, e.g. in the calculation of the dielectric function, the one-electron approximation is itself questionable. Nevertheless, the ground-state eigenvalues and eigenvectors are in practice associated with single-particle excitation energies and wavefunctions. It is well known [10] that for insulators this approximation leads to band gaps which are usually 30–50% narrower than the experimental values. In spite of this problem, it is often possible to obtain good results for the optical properties within the LDA without taking into account many-body effects [11].

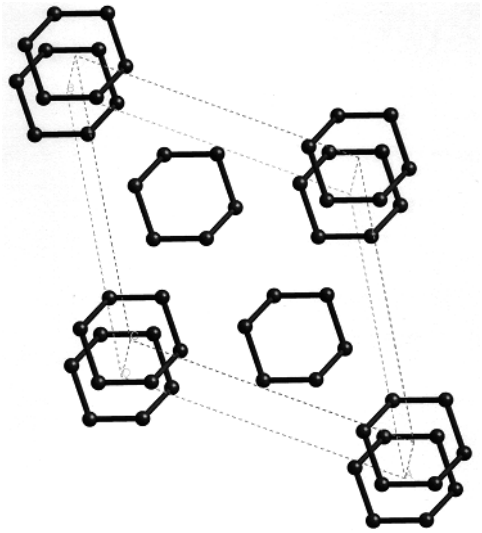

Figure 1. The structure of S_6 [12].

The orthorhombic polymorph of sulphur stable at ambient conditions has 16 S_8 ring molecules per unit cell. This structure is too complex for accurate calculations such as those needed for the determination of the optical properties. Hence, we base our study on the trigonal polymorph with three S_6 ring molecules per unit cell (see figure 1). The trigonal sulphur structure has the space group $R\bar{3}$. In the hexagonal setting, the S atom is located at (0.1454, 0.1882, 0.1055) and the lattice parameters are $a = b = 10.82$ Å, $c = 4.28$ Å [12].

Though the structures of the two polymorphs are different, the gross features of the atomic environment are similar: the interatomic distance is 2.06 Å in the S_8 ring and 2.057 Å in the S_6 ring [13]; the volume per atom is 25.5 Å^3 for S_8 [14] and 23.6 Å^3 for S_6

[12]. Bearing in mind that the 3p orbitals of sulphur are spatially localized, we expect the splittings of the 3p bands in the two polymorphs to be similar. In section 3 we show that this is indeed the case by comparison of the measured x-ray photoemission (XPS) and x-ray emission (XES) spectra with calculated density-of-states (DOS) curves. Thus we expect the main features of the optical properties of the orthorhombic sulphur to be understandable by studying the S_6 polymorph. To our knowledge there have been no *ab initio* calculations of the energy band structures and optical spectra for S_8 and S_6 crystals, and experimental data are available only for the orthorhombic polymorph.

2. Computational details

In order to solve the Schrödinger equation we have used the self-consistent semi-relativistic extended linear augmented-plane-wave method. The formalism of the ELAPW method has been described elsewhere [15]. In the present work we do not take into account the deviations of the one-electron crystal potential from the muffin-tin form. The exchange–correlation potential was constructed following Hedin and Lundqvist [16]. The electron wavefunction was a linear combination of 1467 energy-independent augmented plane waves (APWs) and 8 localized functions per sphere of angular momenta up to $l_{max} = 1$. The augmentation of the basis function was performed by replacing the Bessel function in the angular momentum expansion of the plane waves inside the muffin-tin spheres with the solutions of the radial Schrödinder equation for the singular potential for all $l \leqslant 20$. The plane-wave cut-off was $|\boldsymbol{G}_{max}|r = 6.1$, with $\boldsymbol{G}_{max}$ being the longest reciprocal-lattice vector used in the APW set; $r = 1.028$ Å is the radius of the muffin-tin sphere. We calculated the energy band structure of sulphur over the energy region from the 3s states to 16 eV above the top of the valence band. All eigenenergies in the interval of interest were converged to within 5 mRyd. The core states were included in the self-consistent procedure and were treated fully relativistically via an atomic-like calculation. In constructing the DOS functions and optical spectra we integrated over the irreducible BZ (the IBZ $= \frac{1}{12}$BZ) using the tetrahedron method [17] with a mesh of 135 $\boldsymbol{k}$-points (384 tetrahedra) in the IBZ.

3. Energy band structure

The electronic structure of orthorhombic sulphur has been experimentally probed by ultraviolet photoelectron spectroscopy (UPS) in the range 7.7–21.2 eV [18], by x-ray photoemission spectroscopy [19, 20], by measuring the x-ray emission Kβ spectrum [21], and the Kβ and $L_{II,III}$ [22] spectra. Semi-empirical molecular orbital (MO) calculations have been performed for S_6 and S_8 molecules [13], and for S_8 molecules [19, 23]. X_α scattered-wave calculations [20] have been used for S_8 molecules to interpret experimental data. These calculations qualitatively agree with the valence band measurements, but unanswered questions remain about the position of the 3s states and the extent of the hybridization of the p and d states.

The computed total and l-projected partial DOS curves are shown in figure 2. All of the theoretical curves are convoluted with a Gaussian of 0.2 eV half-width. The energy zero is taken at the valence band maximum. The present calculations predict S_6 to be an insulator with an indirect forbidden gap of 2.0 eV. The measurements by Peanasky *et al* [6] give the value of the fundamental absorption edge as about 3 eV. As expected, LDA underestimates the forbidden gap by ∼30%. We have found the valence band maximum at the $\boldsymbol{k}$-point $A = 2\pi(0, 0, \pm 1/2c)$, and the conduction band minimum at $Z = 2\pi(0, 1/2a, \pm 1/8c)$. In

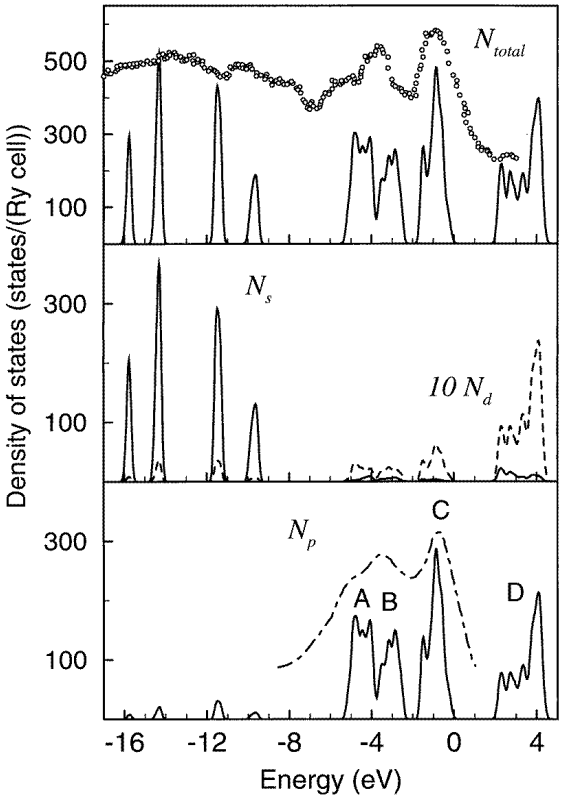

Figure 2. The total and the partial l-projected DOS curves for S_6. In the upper panel the computed total DOS, $N(E)$, is shown by a solid line. The experimentally determined XPS spectrum [19] is represented by circles. In the central panel the solid line denotes the s-projected DOS, N_s. The d-projected DOS, N_d, scaled by a factor of 10, is given by the dashed line. The lower panel shows the calculated p-projected DOS, N_p, by a solid line, while the experimental Kβ XES obtained by Whitehead and Andermann [21] is given as a chain line.

the upper panel of figure 2 the total DOS is compared to XPS data [19]. Taking into account that the measurements were made on S_8, the agreement as regards the energy positions of the main structures in the theoretical and experimental spectra is reasonable.

A broad peak with a width of ∼8 eV centred at 13 eV below the top of the valence band was observed in the $L_{II,III}$ XES spectra by Gusatinskii and Nemnonov [22]. Those results were critically discussed by Nielsen [18], who doubted that the broad peak was due to the 3s states. Our calculated s-projected DOS is presented in the central panel of figure 2. The 3s states in our calculation form 18 bands between −16 and −9.4 eV, which split into four manifolds containing three, six, six, and three bands respectively. The s bands are separated by a gap of ∼4 eV from the valence band. Our calculation predicts the 3s states to be at exactly the energy at which the XES measurement exhibits the unexplained peak. Therefore, we draw the conclusion that it is indeed the 3s states that have been observed in [22].

The valence band consists of 36 bands of predominantly p character. These are shown in the p-projected DOS presented in the lower panel of figure 2. There they are compared to the experimental Kβ XES spectrum of Whitehead and Andermann [21]. The width of the

3p band is 5.4 eV. It consists of the manifolds labelled A, B, C in figure 2. The A manifold contains 12 bands and has a width of ∼1.6 eV. The B manifold contains the next 9 bands and has a width of ∼1.4 eV. These two manifolds slightly overlap, while the C manifold is separated by a gap of ∼0.75 eV. It contains 15 bands and has a width of ∼1.7 eV. The structure of the valence band as well as the energy positions of the main three peaks are in excellent agreement with the Kβ XES spectra of [21, 22].

The 18 lowermost conduction bands (manifold D) are primarily composed of unoccupied 3p states. These bands occupy an energy interval of ∼2.5 eV, which is separated from the upper free-electron-like bands by a gap of ∼0.5 eV. Several authors [19, 13] have discussed the problem of the contribution of the 3d character to the valence and conduction bands. The DOS curves in the central panel of figure 2 show that in our calculation the 3d orbitals strongly contribute to the 3p states, and that their contribution to the unoccupied bands is much larger than that to the occupied bands, though it does not exceed 10%.

4. Optical spectra

The standard theoretical approach in analysing the response of a solid to an external electric field is through a response function. In the case of the optical properties of a solid it is the dielectric function (DF). In the present work we use an *ab initio* approach; in other words we derive the dielectric function from band-structure calculations. This allows us to assign the spectral features to specific excitations in the BZ.

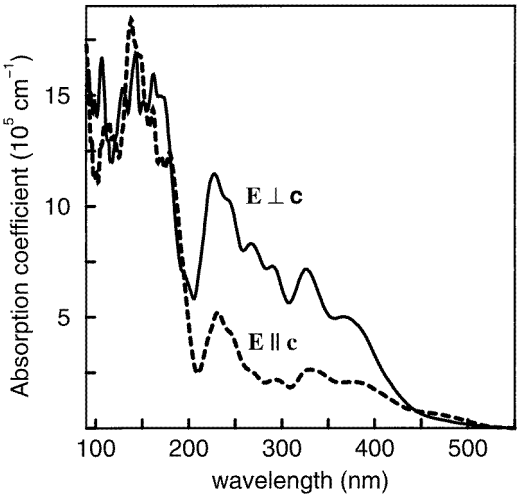

Figure 3. The wavelength dependence of the computed absorption coefficient, α, of S_6 for two light polarizations. The solid line represents α for $\boldsymbol{E} \perp \boldsymbol{c}$, while the dashed line shows α for $\boldsymbol{E} \parallel \boldsymbol{c}$.

The frequency-dependent DF, $\varepsilon(\omega) = \varepsilon_1(\omega) + \mathrm{i}\varepsilon_2(\omega)$, is calculated within the self-consistent-field one-particle approach of Ehrenreich and Cohen [24]. The imaginary part of the dielectric function is given as

$$\varepsilon_2(\omega) = \frac{8\pi^2 e^2}{m^2\omega^2} \sum_i^{occ} \sum_f^{unocc} \int_{BZ} |\boldsymbol{e} \cdot \boldsymbol{P}_{if}|^2 \delta(E_f^{\boldsymbol{k}} - E_i^{\boldsymbol{k}} - \hbar\omega) \frac{\mathrm{d}^3\boldsymbol{k}}{(2\pi)^3} \tag{1}$$

where $\boldsymbol{e}$ is the polarization vector of the electric field, m is the mass of the electron, $\boldsymbol{k}$ is a Bloch vector in the IBZ, E_i and E_f are band energies of the initial and final states. The momentum matrix elements, $\boldsymbol{P}_{if} = \langle \Psi_{\boldsymbol{k}f} | -\mathrm{i}\boldsymbol{\nabla} | \Psi_{\boldsymbol{k}i} \rangle$, were computed as integrals over the unit cell using the formalism described by Krasovskii *et al* [25]. 140 energy bands were considered, of which 54 bands are filled. The fact that the number of bands is finite leads to underestimated values of $\varepsilon_2(\omega)$ for $\hbar\omega > 15$ eV, and to a cut-off of the spectrum at 32 eV. In the energy interval up to $\hbar\omega = 32$ eV the contribution to the f-sum rule [24]

$$\int_0^\infty \varepsilon_2(\omega)\omega \, \mathrm{d}\omega = \frac{2\pi^2 e^2}{m} N_{val}$$

(where N_{val} is the number of the valence electrons) amounts to ~72%. The interband contribution to the spectrum of the real part of the DF, $\varepsilon_1(\omega)$, was calculated by Kramers–Kronig analysis.

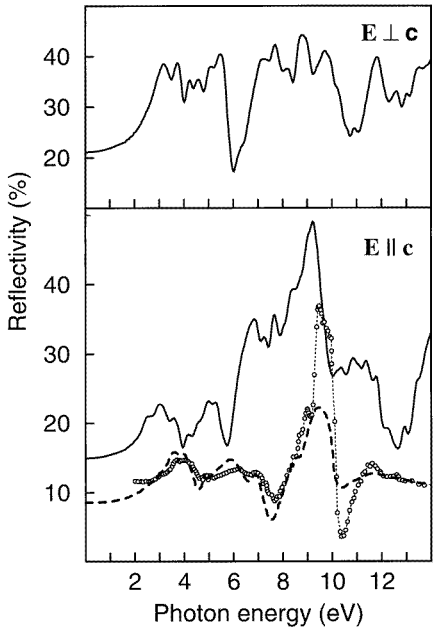

Figure 4. Computed reflectivity spectra of S_6 for two light polarizations. In the upper panel, the solid line represents $\boldsymbol{E} \perp \boldsymbol{c}$ while in the lower panel $\boldsymbol{E} \parallel \boldsymbol{c}$ is given. For comparison the experimental normal-incidence reflectivity spectra for S_8 of Cook and Spear [4] (face (111), circles) and of Emerald *et al* [5] ($\boldsymbol{E} \parallel \boldsymbol{a}$, dashed line) are given.

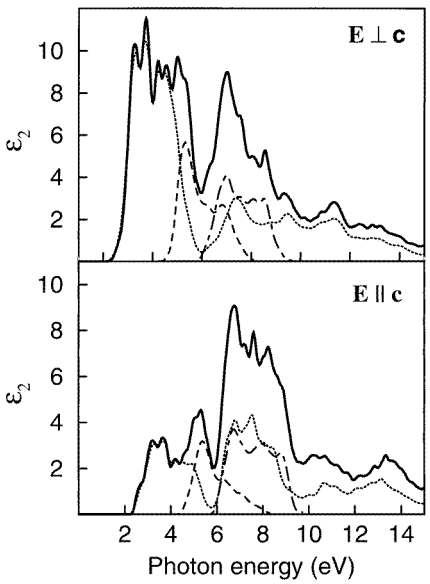

Figure 5. The imaginary part of the dielectric function of S_6 for two light polarizations (solid lines). The contribution of the transitions from manifold A of the valence band (see the text) is indicated by chain lines. Those from manifold B are given by dashed lines, while those from manifold C are represented by dotted lines.

The absorption coefficient, α, and the reflectivity, R, are connected to the DF by

$$\alpha(\omega) = \frac{2\omega}{c} \sqrt{\frac{\sqrt{\varepsilon_1^2(\omega) + \varepsilon_2^2(\omega)} - \varepsilon_1(\omega)}{2}} \tag{2}$$

$$R(\omega) = \left| \frac{\sqrt{\varepsilon(\omega)} - 1}{\sqrt{\varepsilon(\omega)} + 1} \right|^2 . \tag{3}$$

In figure 3 the *ab initio* absorption spectra of S_6 for two light polarizations ($\boldsymbol{E} \parallel \boldsymbol{c}$ and $\boldsymbol{E} \perp \boldsymbol{c}$) are presented. It is seen that the optical properties strongly depend on the polarization. The fundamental absorption edge was found to be larger than the forbidden gap owing to the optical selection rules: 2.29 eV for $\boldsymbol{E} \perp \boldsymbol{c}$ and 2.36 eV for $\boldsymbol{E} \parallel \boldsymbol{c}$, where $\boldsymbol{c}$ is the axis perpendicular to the S_6-ring plane. The yellow colour of sulphur is caused by the steeply increasing absorption in the green-to-violet range of the spectrum (the blue-to-violet range in the experiment [5]). In our calculation it reaches a value of about 10^5 cm^{-1} in the blue region. We observe the strongest absorption for both polarizations between 7.5 and 9.5 eV; the theoretical values of absorption coefficient in this region are between 1.4 and 1.8×10^6 cm^{-1}. The experimental peak [5] is at 9.5 eV and the maximal intensity is about 1.6×10^6 cm^{-1}.

In figure 4 the *ab initio* reflectivity spectra of S_6 in the energy region up to 14 eV for two light polarizations are presented, where they are compared to the reflectivity measurements for S_8 [4, 5]. All of the theoretically predicted structures have counterparts in the measured spectrum shifted by 0.8 eV to higher energies. This is exactly the difference between the theoretical and experimental values of the fundamental absorption edge. The intensity in the experimental spectrum is lower than in the theoretical one because of the unavoidable surface roughness encountered in the experiment. Several authors [3, 19] have interpreted the first peak at $\sim$3.8 eV in the experimental reflectivity spectra as due to Davydov excitons. Our theoretical curve shows this peak at 3 eV. To study its origin we have calculated the initial energy-resolved contributions to ε_2. The result is presented in figure 5. We have found that the structures in the DF spectrum between 2 and 4 eV are determined by the transitions from manifold C to manifold D, the structures between 4 and 6 eV are due to the transitions from manifold B to D, and those between 6 and 10 eV are due to the transitions from A to D, and from C to the free-electron-like states. In summary, all of the transitions are of p $\rightarrow$ p character, each transition resulting from a pair of thin slabs in the BZ parallel to the $z = 0$ plane and symmetric with respect to this plane.

5. Conclusion

This work is an attempt to apply *ab initio* calculations to the interpretation of the experimental optical spectra of sulphur and hence to gain a deeper insight into the origin of its colour. The comparison of experimental data for the orthorhombic polymorph with the results of our calculation for the trigonal one shows that the electronic and optical properties of these two polymorphs are similar. The absorption edge, which determines the colour of sulphur, and all of the structures in the experimental optical spectra in the energy region $0 \leqslant \hbar\omega \leqslant 15$ eV are shown to be due to direct p $\rightarrow$ p interband transitions. In particular, the experimental peak at 3.8 eV seems not to be connected to excitons, as it has its counterpart in the theoretical spectrum.

Acknowledgments

One of the authors (OVK) is grateful for financial support from the Deutsche Forschungsgemeinschaft, DFG, through grant 436 UKR to Professor Klaus Langer, TU Berlin, and BW. Further funding was provided by the DFG to BW (Wi-1232).

References

[1] Burns R G 1993 *Mineralogical Applications of Crystal Field Theory* 2nd edn (Cambridge: Cambridge University Press) p 551

[2] McClure D S 1959 Electronic spectra of molecules and ions in crystals *Solid State Physics* vol 9 (New York: Academic) pp 400–539

[3] Spear W E and Adams A R 1966 Photogeneration of charge carriers and related optical properties in orthorhombic sulphur *J. Phys. Chem. Solids* **27** 281–90

[4] Cook B E and Spear W E 1969 The optical properties of orthorhombic sulphur crystals in the vacuum ultraviolet *J. Phys. Chem. Solids* **30** 1125–34

[5] Emerald R L, Drews R E and Zallen R 1976 Polarization-dependent optical properties of orthorhombic sulfur in the ultraviolet *Phys. Rev.* B **14** 808–13

[6] Peanasky M J, Jurgensen C W and Drickamer H G 1984 The effect of pressure on the optical absorption edge of sulfur to 300 kbar *J. Chem. Phys.* **81** 6407–8

[7] Sasson R, Wright R, Arakawa E T, Khare B N and Sagan C 1986 Optical properties of solid and liquid sulfur at visible and infrared wavelengths *Icarus* **64** 368–74

[8] Hohenberg P and Kohn W 1964 Inhomogeneous electron gas *Phys. Rev.* **136** B864–71

[9] Kohn W and Sham L J 1965 Self-consistent equations including exchange and correlation effects *Phys. Rev.* **140** A1133–7

[10] Godby R W, Schlüter M and Sham L J 1987 Trends in self-energy operators and their corresponding exchange–correlation potentials *Phys. Rev.* B **36** 6497–500

[11] Krasovska O V, Krasovskii E E and Antonov V N 1996 Theoretical study of optical and ultraviolet photoemission spectra of $SrTiO_3$ *Solid State Commun.* **97** 1019–23

[12] Steidel J, Pickardt J and Steudel R 1978 Redetermination of the crystal and molecular structure of cyclohexasulfur, S_6 *Z. Naturf.* b **33** 1554–55

[13] Miller D J and Cusachs L C 1969 Semi-empirical molecular orbital calculations on the bonding in sulfur compounds. I. Elemental sulfur, S_6 and S_8 *Chem. Phys. Lett.* **3** 501–3

[14] Abrahams S C 1955 The crystal and molecular structure of orthorhombic sulfur *Acta Crystallogr.* **8** 661–71

[15] Krasovskii E E 1997 Accuracy and convergence properties of the extended linear augmented-plane-wave method *Phys. Rev.* B **56** 12 866–73 and references therein

[16] Hedin L and Lundqvist B I 1971 Explicit local exchange–correlation potentials *J. Phys. C: Solid State Phys.* **4** 2064–83

[17] Lehman G and Taut M 1972 On the numerical calculation of the density of states and related properties *Phys. Status Solidi* b **54** 469–76

[18] Nielsen P 1974 Photoemission studies of sulfur *Phys. Rev.* B **10** 1673–82

[19] Salaneck W R, Lipari N O, Paton A, Zallen R and Liang K S 1975 Electronic structure of S_8 *Phys. Rev.* B **12** 1493–500

[20] Richardson N V and Weinberger P 1975 The electronic structure of the S_8 molecule *J. Electron Spectrosc. Relat. Phenom.* **6** 109–21

[21] Whitehead H C and Andermann G 1973 An interpretation of the K_β x-ray emission spectra of dibenzyl sulfide and S_8 *J. Phys. Chem.* **77** 721–2

[22] Gusatinskii A N and Nemnonov S A 1969 On the x-ray spectroscopy based derivation of the energy distribution of the density of electron states for the third period elements *Fiz. Tverd. Tela* **11** 1528–36 (Engl. Transl. 1969 *Sov. Phys.–Solid State* **11** 1241–50)

[23] Chen I 1970 Molecular-orbital studies of charge-carrier transport in orthorhombic sulfur. II. Electronic states of the crystal *Phys. Rev.* B **2** 1060–9

[24] Ehrenreich H and Cohen M A 1959 The SCF approach to the many-electron problem *Phys. Rev.* B **115** 789–90

[25] Krasovskii E E, Antonov V N and Nemoshkalenko V V 1990 Microscopic calculation of the interband optical conductivity of ScPd *Phys. Met.* **8** 882–85